Electric-octupole and pure-electric-quadrupole effects in soft-x-ray photoemission

O. Hemmers,[1] S. Oblad,[1] P. Glans,[2] H. Wang,[3] S.B. Whitfield,[4] R. Wehlitz,[5] I.A. Sellin,[6] D.W. Lindle[1], A. Derevianko,[7] and W.R. Johnson,[8]

[1]Department of Chemistry, University of Nevada, Las Vegas, NV 89154-4003, USA
[2]Department of Physics and Mathematics, Mid-Sweden University, 85170 Sundsvall, Sweden
[3]Department of Physics, Uppsala University, Box 530, S-751 21 Uppsala, Sweden
[4]Department of Physics, University of Wisconsin, Eau Claire, WI 54702, USA
[5]Synchrotron Radiation Center, University of Wisconsin, Stoughton, WI 53589, USA
[6]Department of Physics, University of Tennessee, Knoxville, TN 37996, USA
[7]Inst. for Theor. At. and Mol. Phys., Harvard-Smithsonian Center for Astrophysics, Cambridge, MA 02138, USA
[8]Department of Physics, University of Notre Dame, Notre Dame, IN 46556, USA

INTRODUCTION

Second-order [$O(k^2)$, $k=\omega/c$] nondipole effects in soft-x-ray photoemission are demonstrated via an experimental and theoretical study of angular distributions of neon valence photoelectrons in the 100–1200 eV photon-energy range. A newly derived theoretical expression for nondipolar angular distributions characterizes the second-order effects using four new parameters with primary contributions from pure-quadrupole and octupole-dipole interference terms. Independent-particle calculations of these parameters account for a significant portion of the existing discrepancy between experiment and theory for Ne 2*p* first-order nondipole parameters.

THEORY

Second-order [$O(k^2)$] corrections, which arise from interferences between E_1-E_3, E_1-M_2, E_2-E_2, E_2-M_1, M_1-M_1, and from retardation corrections to E_1-E_1 amplitudes, are incorporated into the differential cross section for photoemission as follows:

$$\frac{d\sigma_{n\kappa}}{d\Omega} = \frac{\sigma_{n\kappa}}{4\pi}\left\{\begin{aligned}&1+(\beta_{n\kappa}+\Delta\beta_{n\kappa})P_2(\cos\theta)+(\delta_{n\kappa}+\gamma_{n\kappa}\cos^2\theta)\sin\theta\cos\phi\\&+\eta_{n\kappa}P_2(\cos\theta)\cos 2\phi+\mu_{n\kappa}\cos 2\phi+\xi_{n\kappa}(1+\cos 2\phi)P_4(\cos\theta)\end{aligned}\right\} \quad (1)$$

where the $O(k^2)$-parameters $\Delta\beta$, η, μ, and ξ are introduced [1]. Three of them satisfy the constraint $\eta+\mu+\xi=0$. Reference [1] contains complete formulae and a tabulation of first- and second-order parameters for all subshells of the rare gases helium to xenon.

EXPERIMENT

The experiments were performed with four electron analyzers mounted in a chamber which can rotate about the photon beam [2]. At the nominal angular position of the apparatus, two analyzers are at θ_m [magic angle=54.7°, $P_2(\cos\theta_m)=0$] and $\theta=0°$ in the plane perpendicular to the photon beam $\phi=90°$, which we refer to as the dipole plane because first-order corrections vanish, while two more analyzers are positioned on the forward 35.3° cone with respect to the photon beam (see Fig. 1 inset for definition of angles). At the nominal position, these two "nondipole" analyzers are at (θ_m, $\phi=0°$) and ($\theta=90°$, $\phi=35.3°$). Photoemission intensities in the two magic-angle analyzers are independent of β and can differ only because of nondipole effects. While the magic angle is no longer strictly valid when second-order effects are included, calculations show they can be unimportant in certain geometries.

RESULTS

We present experimental results for Ne γ_{2s} and ζ_{2p} ($=\gamma_{2p}+3\delta_{2p}$) and assuming [$\eta=\mu=\xi=0$ in Eq. (1)], for comparison with *O(k)* and *O(k^2)* calculations. The first data set is based on angle-resolved photoemission intensities from the two magic-angle analyzers. Figure 1 compiles old [3] and new values for γ_{2s} and ζ_{2p} (open squares) determined using this geometry. The solid curves represent *O(k)* calculations [4-6], which agree well with the 2*s* results, but disagree with the 2*p* results above 800 eV. For the magic-angle geometry, Eq. (1) and calculated parameters [1] can be used to estimate *O(k^2)* influences on the experimental determination of γ_{2s} and ζ_{2p}. For example, we predict measured values of ζ_{2p} will be perturbed by second-order effects as follows:

$$\zeta_{2p} = \frac{\gamma + 3\delta + \sqrt{54}(\mu - 7\xi/18)}{1-\mu} \qquad (2)$$

From Eq. (2) and the calculations in [1], effective values for ζ_{2p} (and similarly γ_{2s}) have been determined, yielding the dotted curves in Fig. 1. We find excellent agreement for γ_{2s} and clearly improved agreement for ζ_{2p}. The second-order effects thus included account for much of the difference between first-order theory (solid curve) and experiment for ζ_{2p}, demonstrating the first observation of *O(k^2)* effects in soft-x-ray photoemission.

To confirm this unexpected finding, new measurements in a different geometry were performed by rotating the apparatus to ten different angular positions about the photon beam, yielding 20 angle-resolved intensities for Ne 2*s* and 2*p* photoemission at different angles θ within the dipole plane, and 20 more at different angles θ and ϕ around the 35.3° nondipole cone. From the calculated results for $\Delta\beta_{2p}$, direct second-order effects on β_{2p} should be insignificant; $\Delta\beta_{2p}\approx 0.005$ near 1 keV, smaller than our measurement uncertainties. Therefore, values of β_{2p} determined from the dipole-plane spectra should agree well with DA calculations, if effects due to η, μ and ξ are negligible in the dipole plane. In this plane, we predict their effects will mostly cancel, and thus the excellent agreement [7] between experiment and theory for β_{2p} is not surprising.

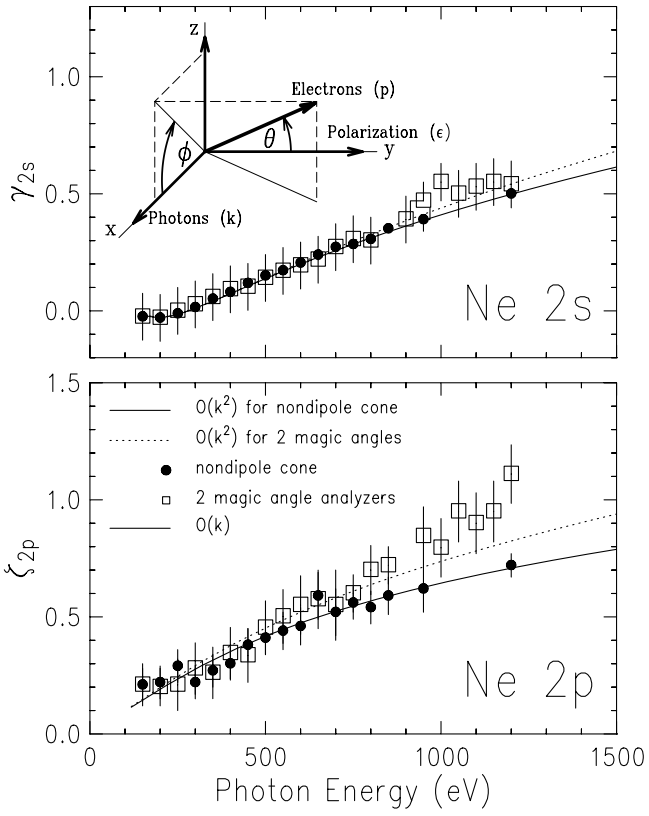

Figure 1. Experimental and theoretical values of γ_{2s} and ζ_{2p} for neon determined under different geometrical conditions: (1) open squares and dotted curve relate to the magic-angle geometry, (2) solid circles and curve relate to the nondipole-cone geometry. Both theoretical curves include effects up to *O(k^2)*. See text for complete description. The solid curve also represents first-order theory, independent of geometry.

In the nondipole cone, however, influences of the *O(k^2)* parameters are superimposed on intensity variations due to the dipole β and the *O(k)* δ and γ parameters. But for both γ_{2s} and ζ_{2p}, our calculations predict effects due to η, μ and ξ also mostly cancel in the nondipole-cone

geometry, yielding the solid curves in Fig. 1. Furthermore, small residual effects around this cone are similar in sign and magnitude for both photolines 2*s* and 2*p*, which is relevant because 2*s*/2*p* intensity ratios are the raw input for data analysis. Assuming no influence of second-order effects in the nondipole cone, we modeled the measured ratios around this cone using Eq. (1) (with $\eta=\mu=\xi=0$) to derive values for γ_{2s} and ζ_{2p}. These results (solid circles in Fig. 1) agree extremely well with O(k) calculations [4-6], confirming our prediction of near cancellation of $O(k^2)$ effects in this geometry.

The experimental geometries described above provide two independent methods to measure γ_{2s} and ζ_{2p}: one relying on measurements using the nondipole analyzers at many angles in the nondipole cone, the other relying on comparison between the (dipole and nondipole) magic-angle analyzers. For the former, we predict $O(k^2)$ effects mostly cancel. For the latter, in contrast, we expect the influences of η, μ, and ξ on Ne 2*p* photoemission to be opposite in sign for $\phi=0°$ and $\phi=90°$, because of the $\cos(2\phi)$ terms in Eq. (1). Thus, second-order effects should be observable only in the latter geometry, hence the differences in measured values of ζ_{2p} shown in Fig. 1.

CONCLUSION

In conclusion, an experimental and theoretical study of neon valence photoemission has demonstrated the first observation of second-order (primarily E_1-E_3 and E_2-E_2) nondipole effects on photoelectron angular distributions in the soft-x-ray region. A general expression for the differential photoionization cross section, including all contributions through second order, has been derived in a form convenient for comparison to experiment.

ACKNOWLEDGMENTS

This work was supported by NSF and DOE EPSCoR. AD and WRJ were supported in part by NSF grant PHY-99-70666. DWL acknowledges UNLV Sabbatical Leave support.

REFERENCES

1. A. Derevianko, W.R. Johnson, and K.T. Cheng, At. Data Nucl. Data Tables **73**, 153 (1999).
2. O. Hemmers, S.B. Whitfield, P. Glans, H. Wang, D.W. Lindle, R. Wehlitz, and I.A. Sellin, Rev. Sci. Instrum. **69**, 3809 (1998).
3. O. Hemmers, P. Glans, D.L. Hansen, H. Wang, S.B. Whitfield, D.W. Lindle, R. Wehlitz, J.C. Levin, I.A. Sellin, R.C.C. Perera, E.W.B. Dias, H.S. Chakraborty, P.C. Deshmukh, and S.T. Manson, J. Phys. B **30**, L727 (1997).
4. J.W. Cooper, Phys. Rev. A **47**, 1841 (1993); **42**, 6942 (1990).
5. A. Bechler and R.H. Pratt, Phys. Rev. A **42**, 6400 (1990); **39**, 1774 (1989).
6. W.R. Johnson, A. Derevianko, K.T. Cheng, V.K. Dolmatov, and S.T. Manson, Phys. Rev. A **59**, 3609 (1999).
7. E.W.B. Dias, H.S. Chakraborty, P.C. Deshmukh, S.T. Manson, O. Hemmers, P. Glans, D.L. Hansen, H. Wang, S.B. Whitfield, D.W. Lindle, R. Wehlitz, J.C. Levin, I.A. Sellin, and R.C.C. Perera, Phys. Rev. Lett. **78**, 4553 (1997).

Principal investigator: Dennis W. Lindle, Department of Chemistry, University of Nevada. Email: lindle@nevada.edu. Telephone: 702-895-4426.

This work is accepted for publication in Phys. Rev. Lett. 2000.